Journal of Alloys and Compounds 509 (2011) 9019–9025

Contents lists available at ScienceDirect

Journal of Alloys and Compounds

journal homepage: www.elsevier.com/locate/jallcom

Calorimetric study of non-isothermal crystallization kinetics of $Zr_{60}Cu_{20}Al_{10}Ni_{10}$ bulk metallic glass

Y.X. Zhuang*, T.F. Duan, H.Y. Shi

Key Laboratory of Electromagnetic Processing of Materials, Ministry of Education, Northeastern University, Shenyang 110819, PR China

ARTICLE INFO

Article history:
Received 26 April 2011
Received in revised form 27 June 2011
Accepted 29 June 2011
Available online 5 July 2011

Keywords:
Crystallization kinetics
Heating rate-dependence
Metallic glass
Non-isothermal process

ABSTRACT

The non-isothermal differential scanning calorimetric techniques were used to evaluate the thermal stability and crystallization kinetics of $Zr_{60}Cu_{20}Al_{10}Ni_{10}$ bulk metallic glass. Various models were used to analyze the non-isothermal DSC at the heating rates (ϕ) ranging from 1 to 80 K/min. The Kissinger equation, Ozawa equation, Augis-Bennett equation, Lasocka equation, and Vogel–Fulcher–Tammann non-linear equation were employed to describe the relationship between the crystallization peak temperatures and the heating rates. The overall crystallization activation energies of the metallic glass were estimated using the Kissinger, Ozawa and Augis–Bennett methods, respectively. The local activation energies at various volume fraction of crystalline phases were obtained by general Ozawa's isoconversional method. The crystallization kinetics was specified by a function reflecting crystallization mechanism. It has been found that a critical heating rate exists at around 20 K/min, beyond which the shapes of the DSC curves and the various relationships are varied. The crystallization process of the metallic glass can be divided into two groups, i.e. a slow heating rates region with ϕ = 1–20 K/min, and a rapid heating rates region with ϕ = 30–80 K/min. The overall crystallization activation energy for the slow heating rates regions is much larger than that for the rapid heating rates region. The crystallization activation energy derived from the Kissinger's peak temperatures is 326.4 ± 11.3 kJ/mol for the slow heating rates region, and 202.2 ± 26.6 kJ/mol for rapid heating rates region, respectively. The crystallization mechanisms were discussed with Johnson–Mehl–Avrami (JMA) and normal grain growth (NGG) mode. The crystallization mechanisms are different for the two heating rates regions. A transition point was found at the NGG-controlled crystallization stage for the higher heating rates, while it was absent for the slower heating rates.

1. Introduction

Metallic glass, as a metastable material at room temperature, crystallizes upon heating. Under an appropriate activation, the atoms rearrange to cause formation of crystalline or quasi-cyrstalline phases. Since the crystallization changes the structures and properties of the metallic glasses, detailed knowledge of the crystallization is very important in understanding the phase transformation far from equilibrium, in controlling the microstructure of the alloys, and in evaluating the thermal stability of the metallic glasses [1].

The crystallization is usually investigated by the techniques of differential scanning calorimetry (DSC), X-ray diffractometry (XRD), ferromagnetic resonance, electrical resistivity and various electron microscopies. Among them, the DSC technique has become a convenient and widely used tool to study the kinetics of the phase transformations. The kinetic data on the phase transformation can be obtained from either the isothermal or non-isothermal scanning heating. The isothermal DSC techniques are in most cases more definitive, while the non-isothermal DSC process has the advantage of having wider temperature range and time-saving. Many phase transformations occur too rapidly to be measured under the isothermal conditions because of short transient time. Meanwhile, industrial processes often depend on the non-isothermal kinetic behavior of the alloys. Therefore, a definitive measurement of the non-isothermal transition kinetics is desirable. Many efforts were given to build up the models to illustrate the non-isothermal crystallization process and thermal stability of various metallic glasses [2–17]. The Johnson–Mehl–Avrami (JMA) formalism, which was developed for determining mechanisms that govern nucleation and growth in the isothermal crystallization process, can also be used for the non-isothermal experiments under certain conditions. The Kissinger's equation is widely used to estimate the overall effective crystallization activation energy [7]. In fact, the non-isothermal crystallization experiments provide the information about the crystallization temperatures, thermal stability, glass forming ability, phase transformation diagrams and crystallization mechanisms of the metallic glasses.

* Corresponding author. Tel.: +86 24 83685996; fax: +86 24 83681758.
E-mail address: yxzhuang@epm.neu.edu.cn (Y.X. Zhuang).

0925-8388/$ – see front matter © 2011 Elsevier B.V. All rights reserved.
doi:10.1016/j.jallcom.2011.06.112

In this work, the crystallization behavior and thermal stability of a Zr-based metallic glass with nominal composition of $Zr_{60}Cu_{20}Al_{10}Ni_{10}$ are investigated using non-isothermal DSC technique. Several equations have been used to illustrate the relationships between the crystallization peak temperatures and the heating rates. We have demonstrated that the non-isothermal crystallization is a heating-rate dependent process. The local activation energies are estimated using Doyle–Ozawa isoconversinal method, and crystallization mechanisms have been discussed in the paper.

2. Theoretical basis

The Kissinger, Ozawa, Augis–Bennett, Lasocka and non-linear Vogel–Fulcher–Tammann (VFT) equations were used in the paper to illustrate the dependence of the crystallization peak temperatures on the heating rates. The Kissinger equation can be written as [7]

$$\ln \frac{T_p^2}{\phi} = \ln \frac{E_c}{R\upsilon} + \frac{E_c}{RT_p} \quad (1)$$

where E_c is the apparent activation energy, R is the universal gas constant, υ is frequency factor, T_p is the peak temperature of crystallization, and ϕ is the heating rate. The equation shows a linear relationship between $\ln(T_p/\phi)$ and $1/T_p$, whose slope is E_c/R. The equation is usually used to estimate the apparent activation energy of the crystallization.

The Ozawa equation [18] has the form of

$$\ln \phi = -\frac{E_c}{RT_p} + C_1 \quad (2)$$

with C_1 as a constant. The equation shows a linear relationship between $\ln\phi$ and $1/T$, and the slope gives the apparent activation energy.

The Augis–Bennett equation [19] is

$$\ln \frac{T_p}{\phi} = \frac{E_c}{RT_p} + \ln K_0 \quad (3)$$

with K_0 as a pre-exponential factor. The equation shows a linear relationship between $\ln(T_p/\phi)$ and $1/T_p$, and the slope results in the apparent activation energy.

The dependence of the characteristic temperature on the heating rate could be also well described using an empirical relationship suggested by Lasocka [20], which is

$$T_p = A + B \ln \phi \quad (4)$$

where A and B are constants for a given material.

Finally, a non-linear VFT equation regarding T and $\ln\phi$ can be expressed as [11]

$$\ln \phi = \ln F - D\frac{T_0}{T_p - T_0} \quad (5)$$

where F is a constant, D is the strength parameter used to describe how closely the system obeys the Arrhenius law, and T_0 is the hypothetical value of the crystallization temperature at the limit of indefinitely slow heating rate.

It is clear that the crystallization activation energy derived from the peak temperatures using the Kissinger, Ozawa, and Augis–Bennett equations is a constant. However, due to the difference of nucleation and growth behavior in the crystallization process, the crystallization activation energy at different volume fraction of crystalline phases (x) might not be a constant. The local activation energy, $E_c(x)$ at different x could be calculated using Doyle–Ozawa isoconversional method [6,21]. The Doyle–Ozawa equation can be expressed as,

$$\ln \phi = -1.0516\frac{E_c(x)}{RT} + C \quad (6)$$

where T is temperature, $E_c(x)$ is the x-dependent activation energy, and C is a constant. Therefore, $E_c(x)$ at a given x can be derived from the slope of $\ln\phi$ versus $1/T$.

It is well known that a general expression for reaction rate of the solid-state reaction is

$$\frac{dx}{dt} = k(T)f(x) \quad (7)$$

where t is the time, $f(x)$ is a function to reflect the crystallization mechanism, and $k(T)$, a temperature dependent rate constant, is determined by Arrhenius relationship, which is

$$k(T) = A\ \exp\left(-\frac{E_c}{RT}\right) \quad (8)$$

where A is frequency factor, and E_c is activation energy for the phase transformation. From Eqs. (7) and (8), we get:

$$\ln\left(\frac{dx}{dt}\right) + \frac{E_c}{RT} = \ln[Af(x)] \quad (9)$$

The right side of the equation is a function related to the crystallization mechanisms $f(x)$. The first item in the left side of the equation can be directly derived from the DSC data, where the heat capacity change contribution should be considered in calculating the volume fraction of crystalline phases [22,23]. Obviously, the function $\ln[Af(x)]$can be evaluated with the known values of activation energy and volume fraction of crystalline phases.

3. Experimental details

Ingot with nominal composition of $Zr_{60}Cu_{20}Al_{10}Ni_{10}$ (at.%) was prepared by arc-melting of 99.9% pure Zr, Al, Ni, and Cu under a titanium-gettered argon atmosphere. The ingot was remelted at least four times to achieve chemical homogeneity. Then, a cylindrical rod with a diameter of 5 mm was prepared by suct-casting into a copper mold under argon atmosphere. The structure of the as-cast samples was characterized by XRD using Cu Kα radiation (PANalytical B.V./X'Pert Pro) diffractometer. The typical broad diffraction maxima in the XRD pattern show fully amorphous characteristics of the as-cast alloy. No crystalline peaks were found within the XRD detection limitation. DSC measurements were performed under a purified argon atmosphere on a TA Q100 at a given heating rate, ϕ. The starting temperature for all the DSC is 303 K. The calorimeter was calibrated for temperature and energy. The value of glass transition temperature (T_g), the onset crystallization temperature (T_x), and the crystallization peak temperature (T_p) were determined with accuracy of ±0.5 K.

4. Results and discussion

A non-isothermal continuous heating DSC trace could give an overview of the crystallization process of the metallic glass at a given heating rate. Fig. 1 shows the non-isothermal DSC traces of the as-cast $Zr_{60}Cu_{20}Al_{10}Ni_{10}$ bulk metallic glass at the heating rates of 1, 2, 5, 10, 20, 30, 40, 60 and 80 K/min. All DSC traces exhibit the endothermic characteristics of a glass transition followed by an exothermic crystallization peak at higher temperature. However, careful examination found that the crystallization peak becomes more asymmetric characterized by an appearing shoulder at higher temperature when the heating rate is larger than 20 K/min. This might suggest that the crystallization process of the bulk metallic glass at higher heating rates differs from that at slower heating rates. The T_g, T_x and T_p of the metallic glass are shifted to higher temperature with the heating rate. The dependence of T_p on the heating rate is re-illustrated in Fig. 2 to give a better view. No linear relationship has been found between T_p and the heating rate (ϕ).

The volume fraction (x) of the crystalline phases during the crystallization event could be evaluated from the DSC curves as a function of temperature at a given heating rate, assuming that the volume fraction x crystallized at temperature T was proportional to the heat released. Therefore, the x at any temperature T is given as $x = A_T/A$ where A is the total area of the whole crystallization peak, and A_T is the partial area between the initial temperature and a given temperature T. However, one should notice that there

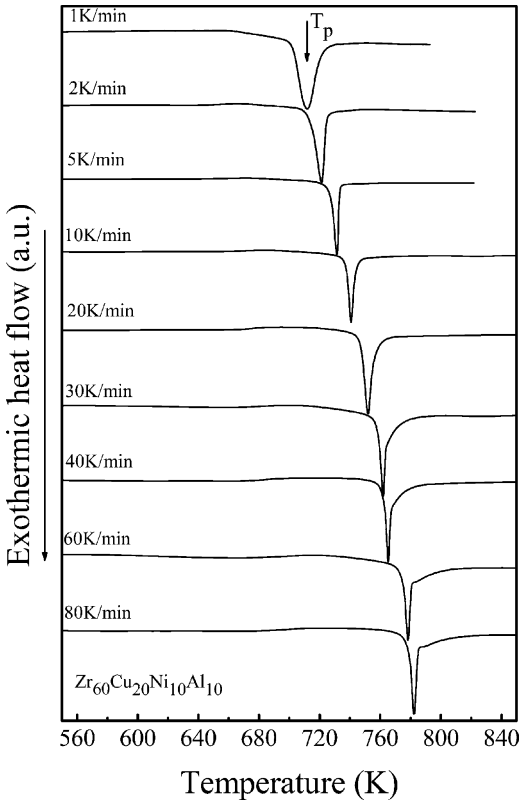

Fig. 1. Non-isothermal DSC traces of as-cast $Zr_{60}Cu_{20}Al_{10}Ni_{10}$ at various heating rate.

is a change of the heat capacity (ΔC_p) of the metallic glass during its exothermic crystallization process. Therefore, the heat capacity change contribution should be considered in calculating the volume fraction from the DSC data using the procedure illustrated in Refs. [22,23]. Fig. 3 displays the crystallized volume fraction of the $Zr_{60}Cu_{20}Al_{10}Ni_{10}$ bulk metallic glass as a function of temperature at different heating rate. Based on their shapes, the curves can clearly be separated into two groups. The five curves at slow heating rates (1, 2, 5, 10 and 20 K/min) have a typical sigmoid type. It have been reported that the sigmoidal plot exhibits the bulk crystallization and excludes the change of surface crystallization [24]. The sigmoid curves have three stages. At first, nucleation occurs at various points in the bulk of the sample and bulk crystallization becomes dominant; then the nuclei grows with a rapid reaction rate since the surface area of nucleation increases; at last, the surface area decreases as a results of nuclei coalesce. However, when the heating rates are between 30 and 80 K/min, the shapes of the crystallized volume fraction are changed. An obvious transition is found when x is between 0.5 and 0.7, from which crystallization rate become slower. It can be concluded that the crystallization of the $Zr_{60}Cu_{20}Al_{10}Ni_{10}$ bulk metallic glass is a heating rate dependent process.

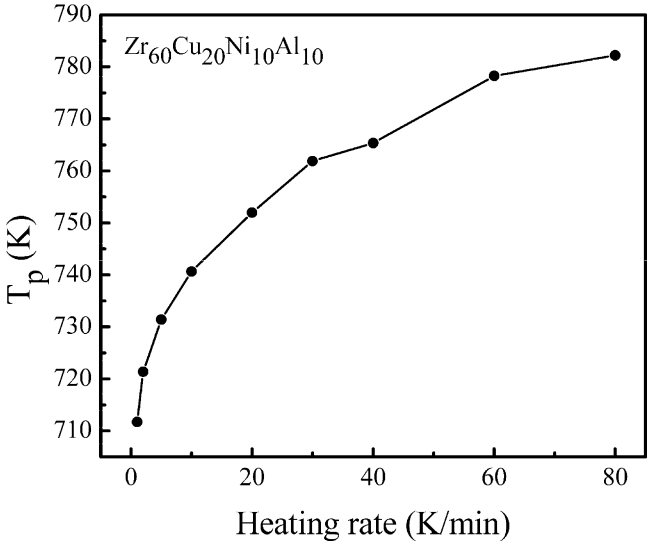

Fig. 2. Dependence of the crystallization peak temperatures of the as-cast $Zr_{60}Cu_{20}Al_{10}Ni_{10}$ bulk metallic glass on the heating rates.

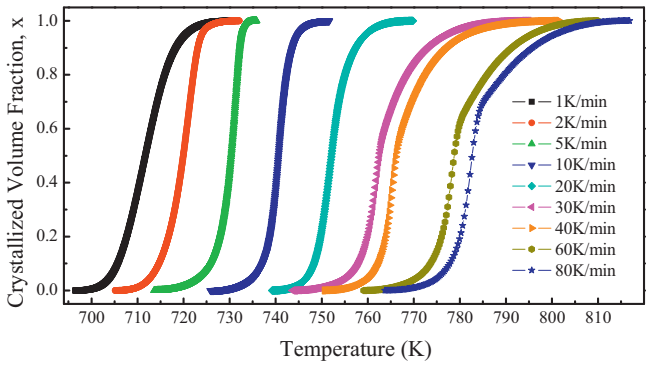

Fig. 3. Crystallized volume fraction (x) as a function of temperature for the $Zr_{60}Cu_{20}Al_{10}Ni_{10}$ bulk metallic glass at different heating rates.

The crystallization peak temperatures at various heating rates can be analyzed using the five equations (Eqs. (1)–(5)) mentioned above. Fig. 4 displays the experimental data in the ways given in Kissinger equation (Fig. 4a), Ozawa equation (Fig. 4b), Augis–Bennett equation (Fig. 4c), Lasocka equation (Fig. 4d) and VFT non-linear equation (Fig. 4e), respectively. It is hard to illustrate the heating rate dependence of T_p using a single linear equation in the whole heating rates range investigated (1–80 K/min), which gives a large deviation between the models and the experimental data. However, if we divide the experimental data into two groups, i.e. the slow heating rates region (1–20 K/min) and the rapid heating rates region (30–80 K/min), the better fitting could be resulted. As shown in Fig. 4a–d, it is clear that the two regions have different slopes, and their intersections could be found at around 20 K/min. Please note that a single VFT equation could well describe the whole experimental data (the dash line in Fig. 4e) in the heating rate range investigated since it is a non-linear equation. The fitting equations for T_p in each region are listed in Table 1 together with the correlation coefficients, r, and the apparent activation energies E_c. The correlation coefficients, r, for all the linear regressions, are better than 0.95, which suggests that the corresponding equations well describe the dependence of the crystallization peak temperatures on the heating rates. It is clear that the slow heating rates region has larger value of slope than the rapid heating rates region as displayed in Fig. 4a–c, meaning that the overall crystallization activation energies in the slow heating rates region are larger than those in the rapid heating rates region. For example, the E_c derived from Kissinger's equation is 326.4 kJ/mol for the continuous heating at 1, 2, 5, 10 and 20 K/min, and 202.2 kJ/mol for the continuous heating at 30, 40, 60 and 80 K/min. The difference between these two values is not within the range of the error. Similar phenomena exist when the Ozawa and Augis–Bennett equations are applied, though larger E_c values have been derived. The results indicate that the overall crystallization activation energy of the as-prepared metallic glass has a strong dependence on the heating rates. When the Lasocka equation is used, a larger slope has been found for the rapid heating rates region.

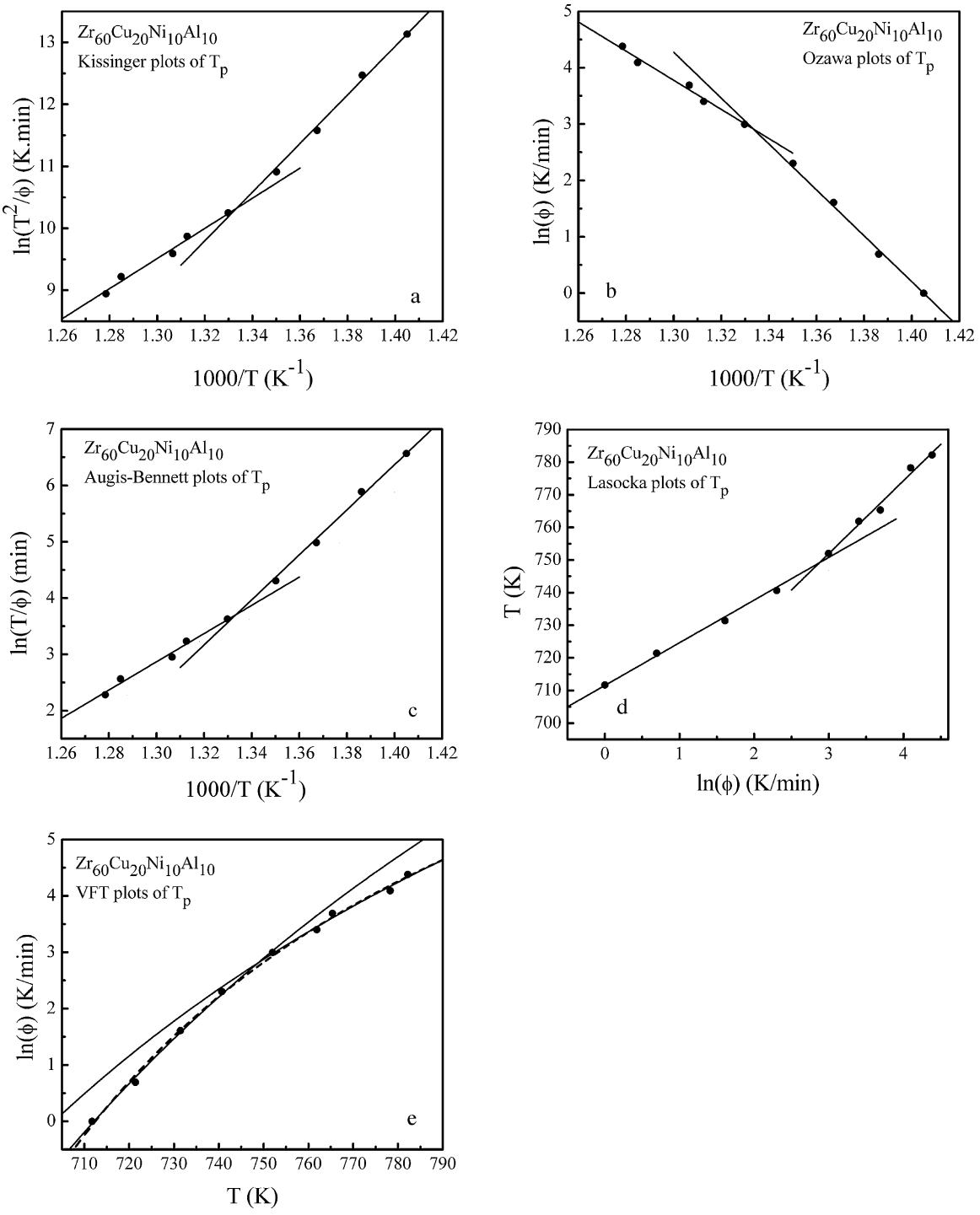

Fig. 4. Kissinger plots (a), Ozawa plots (b), and Augis–Bennett plots (c), Lasocka plots (d), and VFT plots (e) for T_p of the $Zr_{60}Cu_{20}Al_{10}Ni_{10}$ bulk metallic glass. Dots are the experimental data, and solid lines are the corresponding fitting lines.

The constant activation energy derived from peak temperatures could give an overall view about the crystallization process. However, the crystallization activation energy at different x might not be a constant. The local activation energy, $E_c(x)$ at different x calculated using Doyle–Ozawa isoconversional method (Eq. (6)) is given in Fig. 5. It is obvious that the variation of $E_c(x)$ is clearly different in the two heating rates regions. As shown in Fig. 5a, when the heating rates are between 1 and 20 K/min, the local activation energy gradually increases from 292 kJ/mol at $x = 0.04$ to 325 kJ/mol at $x = 0.78$. Afterwards, as crystallization proceeds, $E_c(x)$ decreases with x and reaches a value of 305.5 kJ/mol at $x = 0.99$. However, when the heating rates are between 30 and 80 K/min, the local activation energy decreases from 216 kJ/mol at $x = 0.03$ to 207 kJ/mol at $x = 0.42$, and then increases again to 216 kJ/mol at $x = 0.66$. Considering the error range, we could say that the activation energy is a constant when x is less than 0.66. As the crystallization proceeds, $E_c(x)$ decreases again with x exceeding 0.66, and reaches 188 kJ/mol at $x = 0.95$ (see Fig. 4b). The average value of the activation energy is 310.3 kJ/mol in the slow heating rates region and 207.1 kJ/mol in the rapid heating rates region, respectively. These two values are smaller than those obtained from Ozawa peak method for the corresponding heating rates regions. It can be concluded that the heating rate has an obvi-

Table 1
Relationships between T_p and ϕ fitted using various methods, correlation coefficient (r), and apparent activation energies estimated (E_c).

	Expressions	r	E_c (kJ/mol)
Kissinger equations	Slow heating rates : $\ln T_p^2/\phi = -42.02 + 39256.75/T_p$	0.995	326.4 ± 11.3
	Rapid heating rates : $\ln T_p^2/\phi = -22.10 + 24316.93/T_p$	0.950	202.2 ± 26.6
Ozawa equations	Slow heating rates : $\ln\phi = 57.21 - 40719.6/T_p$	0.996	338.5 ± 11.3
	Rapid heating rates : $\ln\phi = 37.40 - 25860.75/T_p$	0.955	215.0 ± 26.6
Augis–Bennett equations	Slow heating rates : $\ln(T_p/\phi) = -49.62 + 39988.18/T_p$	0.995	332.46 ± 11.3
	Rapid heating rates : $\ln(T_p/\phi) = -29.75 + 25088.84/T_p$	0.952	208.60 ± 26.6
Lasocka equations	Slow heating rates : $T_p = 711.54 + 13.09\ln(\phi)$	0.994	
	Rapid heating rates : $T_p = 684.93 + 22.35\ln(\phi)$	0.955	
VFT equations	Slow heating rates : $\ln\phi = \ln(3.403\times10^9) + 11.81\times463.1/(T_p - 463.1)$		
	Rapid heating rates : $\ln\phi = \ln 127197.5 + 2.354\times593.5/(T_p - 593.5)$		

ous effect on the local activation energies of the $Zr_{60}Cu_{20}Al_{10}Ni_{10}$ bulk metallic glass.

According to Eq. (9), the function $\ln[Af(x)]$, which reflects the crystallization mechanisms, could be estimated using the known values of activation energy and volume fraction of crystalline phase (Fig. 3). Fig. 6a and b displays the experimental data (open circles) of the function $\ln[Af(x)]$ as a function of x in the slow heating rates region and the rapid heating rates region, respectively. The experimental data plotted in Fig. 6 are the average values corresponding to the same crystallized volume fraction at each heating rate in the same region. In the same heating rates regions (the slow heating rates region or the rapid heating rates region), the individual curve for each heating rate has similar shape and trend (not

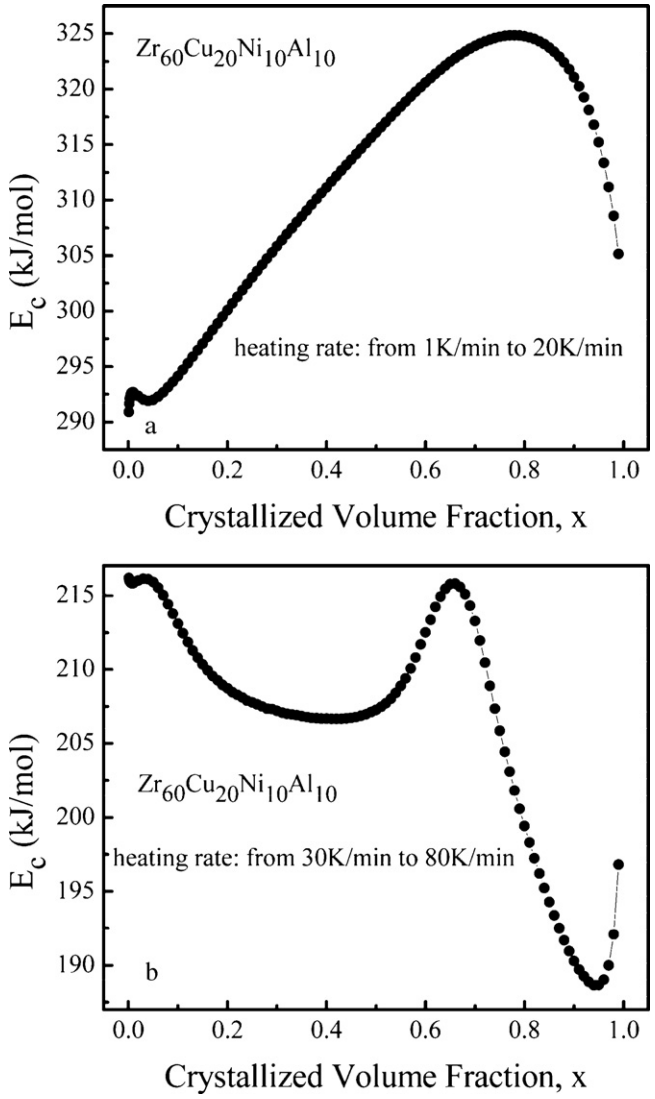

Fig. 5. Local activation energies as a function of crystallized volume fraction for continuous heating crystallization at heating rates of 1–20 K/min (a) and 30–80 K/min (b).

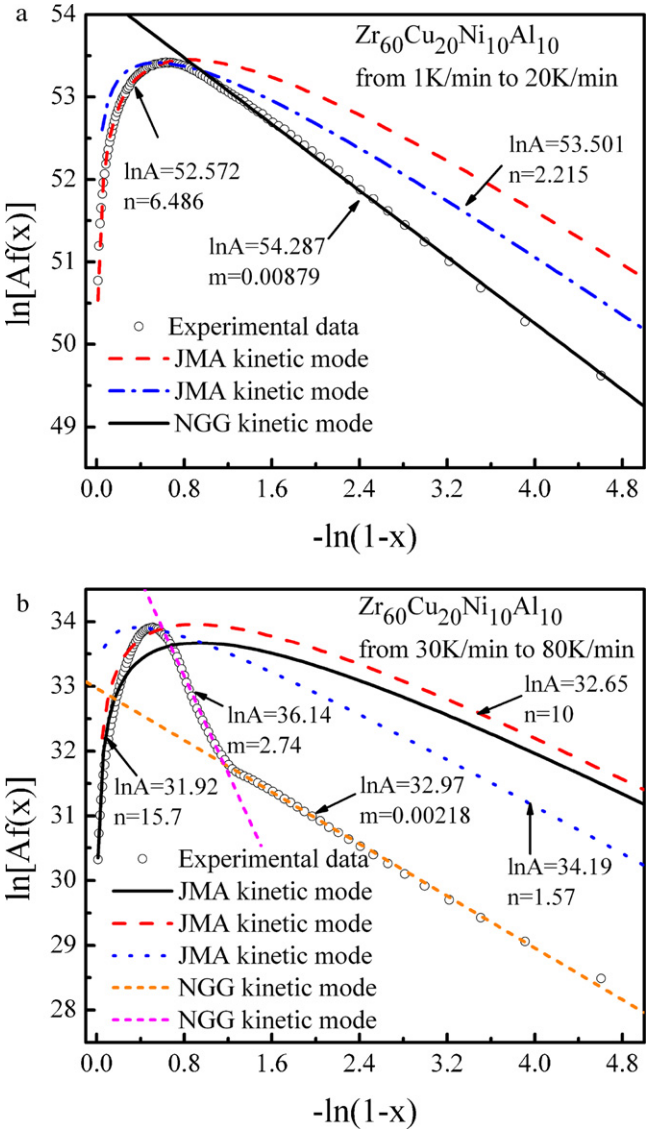

Fig. 6. Curves reflecting crystallization mechanisms of $Zr_{60}Cu_{20}Al_{10}Ni_{10}$ bulk metallic glass in the slow heating rates region (a) and in the rapid heating rates region (b).

Table 2
Theoretical kinetic model equations considered.

Model	$f(x)$	Label
Johnson–Mehl–Avrami (JMA)	$n(1-x)[-\ln(1-x)]^{(n-1)/n}$	n
Normal grain growth (NGG)	$(1-x)^{m+1}$	m

shown here), indicating that the crystallization mechanism keep same in the same heating rates region. As shown in Fig. 6, the shapes of the function $\ln[Af(x)]$ in the two heating rates regions are obviously different, suggesting that the crystallization mechanisms are different for the two heating rates regions. When the heating rates lie between 1 and 20 K/min, the function $\ln[Af(x)]$ rapidly increases at the beginning of the crystallization, and reaches its maximum (53.4) at x is 0.45. Then, the function $\ln[Af(x)]$ gradually decreases followed by a linear decrease when $x > 0.64$. When the heating rates are from 30 K/min to 80 K/min, the function $\ln[Af(x)]$ rapidly increases at the beginning of the crystallization, and reaches its maximum (33.9) at x is 0.40. With the crystallization proceeding, the $\ln[Af(x)]$ linearly decreases to 31.8 at $x = 0.69$ followed by another linear decrease with a smaller slope. The value of $\ln[Af(x)]$ at various x in the two regions are significantly different. Besides this, a transition point could be found at the advanced crystallization stage for the higher heating rate, while it was absent for the slower heating rate.

Using the least-squares minimization curve fitting procedure, the experimental data (open circles in Fig. 6) was analyzed using Johnson–Mehl–Avrami (JMA) and normal grain growth (NGG) models. The expressions of the two models [25] are listed in Table 2. In the slow heating rates region as shown in Fig. 6a, the crystallization begins with the JMA-like kinetics having JMA exponent $n = 6.5$ for $x < 0.42$; then n gradually decreases to 2.2 for $0.42 < x < 0.64$; afterwards, the experimental data follows a straight line with NGG exponent $m = 0.0088$ for $0.64 < x < 0.99$. When the heating rates are in the range of 30–80 K/min, the crystallization starts with the JMA-like kinetics having a larger JMA exponent of $n = 15.7$ for $x < 0.22$; then n gradually decreases to 1.57 at x is about 0.43. With the crystallization going on, the experimental data can be described by a straight line with NGG exponent $m = 2.74$ for $0.43 < x < 0.69$, and followed by another straight line with NGG exponent $m = 0.002$ for $0.69 < x < 0.99$. The crystallization process starts to be described using the NGG model at different x in the two heating rates regions. The NGG model could describe longer process of the crystallization in the rapid heating rates region than that in the slow heating rates region.

The ZrNiCuAl bulk metallic glasses crystallize by simultaneous precipitation of Zr_2Ni, Zr_2Cu, $Cu_{10}Zr_7$ and other crystalline phases. The variation of the local activation energy $E_c(x)$ with x in both heating rates regions indicates that the crystallization of the metallic glass has a complex mechanism, which is composed of the JMA-like mode in the initial stage of the crystallization and the NGG-like mode at the advanced stage of the process. The JMA model represents the nucleation and growth of the crystalline phase in the metallic glass. The JMA exponent with a value larger than 4 implies the crystallization characterized by a increasing nucleation rate with the time and interface-controlled three-dimension growth; while a value of 1.5–2.5 implies a diffusion-controlled three-dimension growth with a decreasing nucleation rate with time. In the initial crystallization stage, n is 6.5 for the slow heating rates region, and larger n value of 15.7 for the rapid heating rates region, which might indicate that the initial nucleation rate in the slow heating rates region is slower than that in the rapid heating rates region. At the advanced stage of the crystallization, the process is characterized by NGG-kinetics. In the slow heating rates region, the NGG-kinetics becomes dominant when x reaches 0.64, while the NGG growth mode dominates over the JMA mode when x is 0.43 in the rapid heating rates region, meaning that the JMA-like mode could describe longer process of the crystallization in the slow heating rates region than that in the rapid heating rates region. The phenomenon has also been found in the non-isothermal crystallization process of $Co_{43}Fe_{20}Ta_{5.5}B_{31.5}$ metallic glass [25]. When a glass is heated at a constant rate, crystal nuclei are formed only at lower temperatures and crystal particles grow at higher temperatures [26]. Thus, when the heating rate is slow, there is relatively sufficient time for crystal nucleation occurring at lower temperature. An interesting phenomenon is that there is an obvious transition at x around 0.69 when the heating rates lie in the range between 30 and 80 K/min, from which a NGG exponent becomes much smaller. This might be related to the change of growth rate and surface area. However, the real reason is still an open question.

5. Conclusions

The non-isothermal DSC measurements were conducted at nine heating rates of 1, 2, 5, 10, 20, 30, 40, 60 and 80 K/min to investigate the crystallization kinetics and thermal stability of the $Zr_{60}Cu_{20}Al_{10}Ni_{10}$ bulk metallic glass. Several models have been used to analyze the non-isothermal DSC traces. The following results were derived.

(1) The relationships between the crystallization peak temperatures and the heating rates cannot be described using a single linear equation in the whole heating rates investigated. However, when a single VFT non-linear equation is used, a reasonable good fitting can be obtained
(2) The crystallization of the bulk metallic glass is a heating rate-dependent process. A critical heating rate exists at around 20 K/min, beyond which the shapes of the DSC traces, the heating rate dependences of the crystallization temperatures, the activation energies, the variation of local activation energy with crystallized volume fraction, and the crystallization mechanisms are changed. The used heating rates can be grouped as the slow heating rates region with the heating rate changing from 1 to 20 K/min, and the rapid heating rates region with the heating rates ranging from 30 to 80 K/min.
(3) The crystallization activation energies of the Zr-based metallic glass are 326.4, 338.5, 332.5, and 310.3 kJ/mol for the slow heating rates region, and 202.2, 215.0, 208.60 and 207.1 kJ/mol for the rapid heating rate region, when the Kissinger's peak temperature, Ozawa' peak temperature and Augis–Bennett's peak temperature, and Ozawa's isoconversional method were employed, respectively.
(4) The crystallization of the metallic glass has a complex mechanism, which is composed of the JMA-like mode in the initial stage of the crystallization and the NGG-like mode at the advanced stage of the process. A transition point was found at the NGG-controlled crystallization stage for the higher heating rates, while it was absent for the slower heating rates.

Acknowledgement

The author (Y.X. Zhuang) is grateful to the financial support of the Fundamental Research Funds for the Central University (Grant No. N100409001).

References

[1] W.H. Wang, C. Dong, C.H. Shek, Mater. Sci. Eng. R 44 (2004) 45.
[2] E. Illekova, Thermochim. Acta 387 (2002) 47.
[3] K.N. Lad, R.T. Savalia, A. Pratap, G.K. Dey, S. Banerjee, Thermochim. Acta 473 (2008) 74.
[4] F. Liu, F. Sommer, E.J. Mittemeijer, J. Mater. Sci. 39 (2004) 1621.

[5] K. Matusita, S. Sakka, Phys. Chem. Glasses 20 (1979) 77.
[6] T. Ozawa, Bull. Chem. Soc. Jpn. 38 (1970) 1881.
[7] H.E. Kissinger, Anal. Chem. 29 (1957) 1702.
[8] D.V. Louzguine, A. Inoue, Appl. Phys. Lett. 81 (2002) 2561–2562.
[9] Y.X. Zhuang, W.H. Wang, Y. Zhang, M.X. Pan, D.Q. Zhao, Appl. Phys. Lett. 75 (1999) 2392–2394.
[10] Y.X. Zhuang, W.H. Wang, J. Appl. Phys. 88 (2000) 8209.
[11] L. Xia, D. Ding, S.T. Shan, Y.D. Dong, Appl. Phys. Lett. 90 (2007) 111903.
[12] J. Bonastre, L. Escoda, J. Saurina, J.J. Sunol, J.D. Santos, M.L. Sanchez, B. Hernando, J. Non-Cryst. Solids 354 (2008) 5126.
[13] J.L. Cardenas-Leal, J. Vazquez, P.L. Lopez-Alemany, P. Villares, R. Jimenez-Garay, J. Alloys Compd. 471 (2009) 44–51.
[14] J.S.C. Jang, S.F. Tsao, L.J. Chang, J.C. Huang, C.T. Liu, Intermetallics 17 (2009) 56–64.
[15] D. Qiao, C. Fan, P.K. Liaw, H. Choo, Adv. Eng. Mater. 8 (2006) 714.
[16] J. Zhu, M.T. Clavaguera-Mora, N. Clavaguera, Appl. Phys. Lett. 70 (1997) 1709.
[17] N. Mitrovic, S. Roth, J. Eckert, Appl. Phys. Lett. 78 (2001) 2145.
[18] T. Ozawa, J. Therm. Anal. 2 (1970) 301.
[19] J.A. Augis, J.E. Bennett, J. Therm. Anal. 13 (1978) 283.
[20] M. Lasocka, Mater. Sci. Eng. 23 (1976) 173.
[21] R.Z. Hu, Q.Z. Shi, Thermal Analysis Kinetics , Science Press, Beijing, China, 2001, pp. 25–44.
[22] Y.X. Zhuang, P.F. Xing, H.Y. Shi, J. Chen, P.W. Wang, J.C. He, J. Appl. Phys. 108 (2010) 033515.
[23] N. Clavaguera, M.T. Clavaguera-Mora, M. Fontana, J. Mater. Res. 13 (1998) 744.
[24] A. Pratap, K.N. Lad, T.L.S. Rao, P. Majnudar, N.S. Saxena, J. Non-Cryst. Solids 345–346 (2004) 178.
[25] Z.Z. Yuan, X.D. Chen, B.X. Wang, Y.J. Wang, J. Alloys Compd. 407 (2006) 163.
[26] K. Matusita, T. Komatsu, R. Yokota, J. Mater. Sci. 19 (1984) 291.